ELSEVIER

Materials Science and Engineering A333 (2002) 60–66

MATERIALS SCIENCE & ENGINEERING A

www.elsevier.com/locate/msea

Model for the maximum fraction of retained austenite in austempered ductile cast iron

M.A. Yescas, H.K.D.H. Bhadeshia *

Department of Materials, Science and Metallurgy, University of Cambridge, Pembroke Street, Cambridge, CB2 3QZ, UK

Received 21 June 2001; received in revised form 30 August 2001

Abstract

Austempered ductile irons usually contain a large quantity of retained austenite that can help to optimise their mechanical properties. A generic model has been created that enables the estimation of the maximum fraction of retained austenite as a function of the chemical composition and heat treatment. It is found that the maximum fraction of retained austenite depends on two competing effects. The first is that austenite is stabilised by transforming to bainite at lower temperatures, since, consistent with the T_0 curve, the limiting carbon concentration of the austenite increases as the transformation temperature is reduced. The counteracting effect is that the formation of bainitic ferrite itself consumes austenite, so less is available for retention on cooling to ambient temperature. The model has been validated by comparison with experiments on homogenised samples of cast iron.

Keywords: Retained austenite; Austempered; Ductile iron; Bainite; Carbon concentration

1. Introduction

A wide range of properties can be produced in austempered ductile irons by changing the heat treatment conditions and hence, the microstructure [1]. A mixture of bainitic ferrite and retained austenite (V_{γ_r}), along with graphite nodules, is the most desirable combination of phases in these cast irons. Undesirable phases, such as martensite and iron carbides, may also be present in smaller quantities, but it is understood that the maximisation of retained austenite is important towards the achievement of good mechanical properties [2].

The heat treatment consists of austenitisation, normally in the range 850–950, followed by isothermal transformation in the temperature range where bainite is expected (usually 250–450 °C). When discussing the microstructure, it is necessary to distinguish between residual austenite, which exists at the isothermal transformation temperature and retained austenite, which remains untransformed at ambient temperature. Carbon is partitioned into residual austenite during the bainite transformation. However, this partitioning occurs after the diffusionless growth of each bainite plate [3,4], so that the transformation cannot occur if diffusionless growth is thermodynamically not possible. At some stage in the evolution of the microstructure, the austenite carbon concentration reaches the T_0 curve, at which point bainite ceases to form, assuming a homogeneous distribution of carbon in the austenite. The T_0 curve is the locus of all points on the temperature versus carbon concentration plot, where austenite and ferrite of the same chemical composition have identical free energies. The reaction is said to be incomplete, since it stops before the austenite has achieved its equilibrium composition [5,6] given by the Ae_3 curve, (Fig. 1). Naturally, it is at this stage that the retained austenite is most stabilised by carbon that has reached its maximum permissible concentration in the context of bainite.

In previous work [7], a vast quantity of experimental data on retained austenite in cast irons, compiled from the published literature, was assessed and expressed quantitatively using neural network analysis. This is a method of empirical non-linear regression analysis.

---

* Corresponding author. Tel.: +44-122-333-4301; fax: +44-122-333-4567.
E-mail address: hkdb@cus.cam.ac.uk (H.K.D.H. Bhadeshia).

PII: S0921-5093(01)01840-8

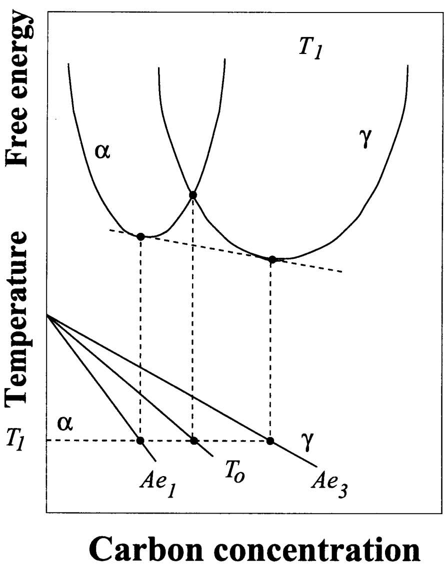

Fig. 1. Schematic illustration of the origin of the T_0 curve on the phase diagram. α and γ refer to ferrite and austenite, respectively.

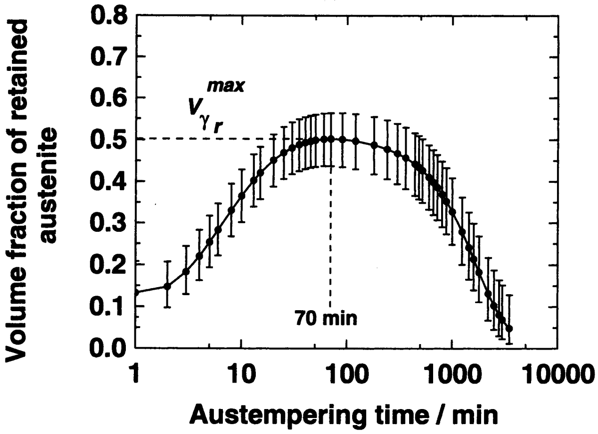

Fig. 2. Variation of the volume fraction of retained austenite as a function of austempering time, calculated using a published model [7]. In this case, the time required to achieve the maximum fraction at 380 °C is 70 min. The error bars represent uncertainty in the calculated results [7].

The purpose of the present work was to create a mechanism-based model capable of estimating the maximum volume fraction of retained austenite in austempered ductile irons, as a function of the chemical composition and heat treatment.

2. Experimental procedures

A ductile cast iron produced in a commercial foundry using electric melting has been used for the experiments. Its chemical composition is Fe–3.55C–2.5Si–0.55Mn–0.15Mo–0.31Cu (wt.%). Solid cylindrical specimens with dimensions 8 mm diameter and 12 mm length were machined from a keel block. Samples were first homogenised at 1000 °C for 3 days in a carbolite furnace, whilst sealed in quartz tubes containing argon, before quenching in water.

Austempering was performed in a thermomechanical simulator ('Thermec-mastor Z') which is capable of implementing specified thermal cycles on small samples and of recording temperature and dilatation as a function of time. The samples were austenitised for 15 min at 950 °C; they were then quenched to the isothermal temperature and held there for a specific period of time. This time period was intended to be that required to obtain the maximum volume fraction of retained austenite ($V_{\gamma_r}^{max}$), as estimated using a model previously developed [7]. Fig. 2 shows how the volume fraction calculated using that model varies with austempering time t_A, enabling the required time to be selected for each austempering temperature T_A (Table 1). Transmission electron microscopy analysis was carried out in samples austempered at 250 °C for 50 and 90 min, respectively following austenitisation at 950 °C for 30 min.

The volume fraction or retained austenite (V_{γ_r}) was measured using X-ray diffraction [8] with CuK_α radiation at 40 kV and 40 mA. A Phillips diffractometer was used with a step-scan mode to cover the angular 2θ range from 47 to 103°. The 2θ step size was 0.03° with a dwell time of 30 s. Three peaks of ferrite (001, 112, 022) and three of austenite (002, 022, 113) were utilised for this purpose. The carbon concentration in the austenite was calculated from its lattice parameter [8] using a relationship due to Dyson and Holmes [9].

For transmission electron microscopy (TEM), 3 mm diameter discs, 0.5 mm thick, were mechanically polished using 600 grit silicon carbide paper to 0.1 mm

Table 1
Calculated austempering temperatures and times utilised in experiments

T_A (°C)	t_A (min)	T_A (°C)	t_A (min)	T_A (°C)	t_A (min)	T_A (°C)	t_A (min)
250	50	300	63	350	64	400	52
260	55	310	63	360	67	410	40
270	60	320	63	370	70	420	31
280	61	330	63	380	70	430	23
290	63	340	63	390	63	440	17

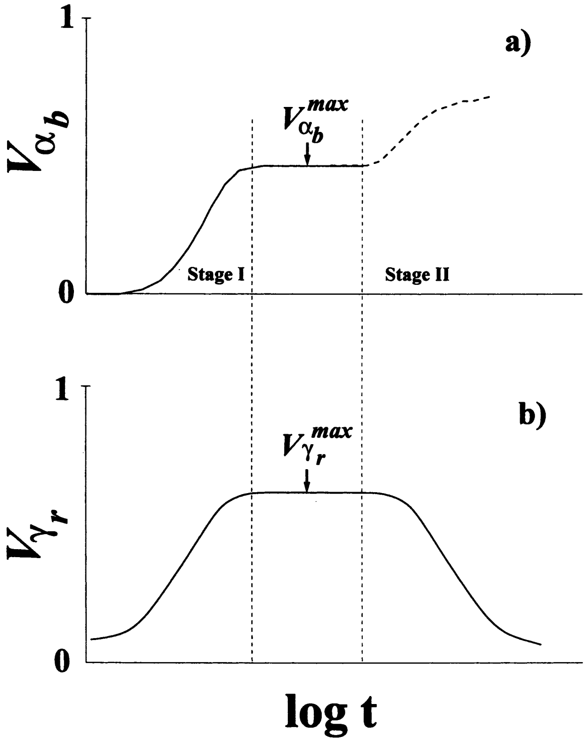

Fig. 3. Schematic representation of (a) bainitic ferrite and (b) retained austenite, as a function of time. V_{α_b} and V_{γ_r} represent the volume fractions of bainitic ferrite and retained austenite, respectively.

thickness. A precision dimple grinder instrument was used prior to milling with two argon-ion guns. The angle between the ion beams and specimen was set to 10°. Transmission electron microscopy was conducted using a Jeol JEM-200CX electron microscope operated at 200 kV.

3. Variation of retained austenite

The isothermal transformation of cast iron to generate bainite is known as 'austempering'. The process is defined conventionally in two stages [10]. The end of the first stage corresponds to the maximisation of the fraction of bainitic ferrite and the enrichment of the austenite, the second with the onset of carbide precipitation. The time interval between these two stages is the heat treatment window [10,11] (Fig. 3). The effect of austempering can be optimised within the confines of this window: too short an austempering time leads to an inadequate enrichment of the austenite and hence, a low retained austenite content. Austempering beyond the commencement of stage II causes carbide precipitation and hence, a reduction in the retained austenite content (Fig. 3b).

It is known that the extent of transformation to bainite in ductile irons, as in steels, decreases ultimately to zero when increasing the isothermal transformation temperature towards the bainite-start temperature [12]. This is because the austenite can only transform to bainite if its carbon concentration is less than a value x_{T_0} given by the T_0 curve defined earlier. It follows [13] that the distribution of carbon at the point where the bainite reaction stops is given by

$$\bar{x} = V_{\alpha_b} x_{\alpha_b} + V_\gamma x_{T_0} \quad (1)$$

where $\bar{x}$ is the average carbon concentration of the austenite prior to transformation, V_{α_b} and V_γ are the volume fractions of bainitic ferrite and residual austenite, respectively, at the point where the reaction stops. x_{α_b} is the carbon concentration of the bainitic ferrite.

Given that in silicon-rich alloys, such as the cast irons considered here, $V_\gamma = 1 - V_{\alpha_b}$, the maximum fraction of bainitic ferrite is given approximately by

$$V_{\alpha_b}^{\max} = \frac{x_{T_0} - \bar{x}}{x_{T_0} - x_{\alpha_b}} \quad (2)$$

Since x_{T_0} is the carbon concentration of the residual austenite, its value can be used to calculate the martensite-start (M_S) of that austenite. If M_S falls below room temperature, the austenite is retained completely. The maximum volume fraction of retained austenite $V_{\gamma_r}^{\max}$ will then equal $1 - V_{\alpha_b}^{\max}$ which is calculated using Eq. (2). On the other hand, if M_S exceeds room temperature, $V_{\gamma_r}^{\max}$ can be calculated using the relationship first introduced by Koistinen and Marburger [14], which describes the progress of athermal martensitic transformation in a sample which is initially fully austenitic:

$$1 - V_{\alpha'} = \exp(-C_1[M_S - T]) \quad (3)$$

where $V_{\alpha'}$ is the volume fraction of martensite and C_1 is a constant obtained originally by fitting to experimental data. For the present purposes, where we wish to determine the austenite retained, T is set to 20 °C.

For a specimen which is initially fully austenitic, the term $(1 - V_{\alpha'})$ in Eq. (3) is equal to $V_{\gamma_r}^{\max}$ because it represents the volume fraction of austenite which does not transform to martensite.

An alternative relationship due to Khan and Bhadeshia [13], based on the effect of autocatalytic nucleation is given by

$$-\ln(1 - V_{\alpha'})/V_{\alpha'} = 1 + C_2[M_S - T] \quad (4)$$

where $C_2 = 0.0029$ is another fitting constant and the temperatures are expressed in °C or Kelvin.

It has been pointed out in previous work [3,15] and shown in Fig. 4 that the concentration of carbon in the austenite may not be limited exactly by the T_0 line when the distribution of carbon in the austenite is not uniform. Indeed, studies specific to cast iron using X-ray diffraction, by Niesawaah and Hijhof [16], Ahmadabadi [17] and Chang [18] have shown that the average carbon concentration in the retained austenite tends to be slightly higher than indicated by the T_0 curve. Part of the reason is that in a heterogeneous sample, X-ray diffraction tends to over-estimate the carbon concentration, since it is only the high-carbon regions of austenite that are retained [19].

It is necessary to take account of the transition from upper to lower bainite in cast irons [22]. It is assumed here that the transition temperature is ≈ 350 °C [23,24]. The carbon content of upper bainitic ferrite was considered to be 0.03 (wt.%) [20]. For lower bainite, the carbon locked in the ferrite, as carbides must increase as the transformation temperature is reduced; this is discussed in the next section.

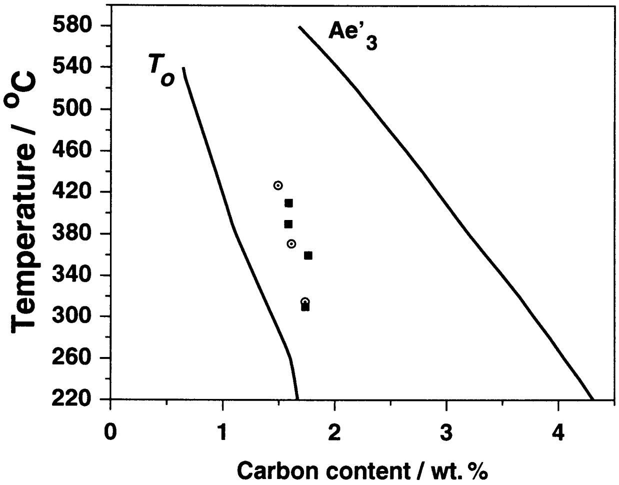

Fig. 4. The calculated [20] T_0 and paraequilibrium Ae'_3 curves for Fe–3.5C–2.5Si–0.55Mn–0.15Mo–0.31Cu (wt.%). Experimental values of x_γ are also shown. Squares correspond to the iron used for T_0 and Ae'_3 lines, whereas the open circles are for a similar iron studied by Rundman [21] (Fe–3.5C–2.1Si–0.5Mn–0.71Mo wt.%).

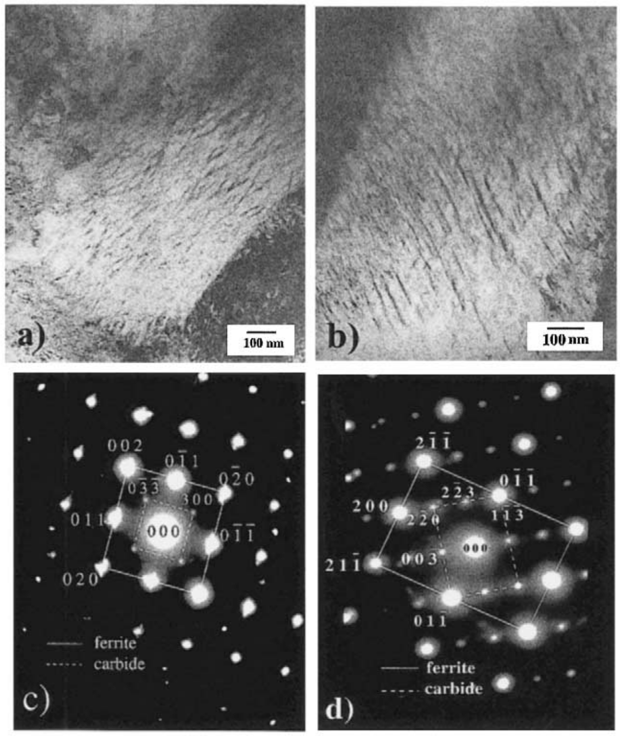

Fig. 5. TEM micrographs showing brightfield images of (a) τ carbides and (b) silicon-rich carbides of the type (Fe,Si)C_x. Selected area electron diffraction patterns of (c) τ and (d) silicon-rich carbides.

3.1. Carbon in lower bainite

Epsilon (ε) and other transition carbides often occur in lower bainite in high-carbon high-silicon steels [25,26], as well as in ADI [27–29]. The detection of these carbides in lower bainite is important in that it demonstrates that part of the carbon is not available for partitioning into the residual austenite. The presence of transition carbides may also imply the retention of a high carbon concentration in solution in the ferrite. Thus, Roberts [30] reported a stable, dissolved carbon to a concentration of ≈ 0.25 (wt.%) during the precipitation of ε carbide. Kang [31] made in situ observations using hot-stage transmission electron microscopy of the precipitation of carbides within lower bainite and reported a supersaturation of the order of 0.3 (wt.%) for a high-silicon steel transformed to bainite at 310 °C.

During the present investigation, carbides were found within bainitic ferrite for non-homogenised austempered ductile iron Fe–3.5C–2.5Si–0.55Mn–0.15Mo–0.31Cu (wt.%) austenitised at 950 °C and austempered at 250 °C for 50 and 90 min. Fig. 5(a) shows a brightfield image of carbides for which a diffraction pattern is shown in Fig. 5(c). Ahmadabadi [29] found the same diffraction pattern, though he did not index it. The pattern could not be indexed to other carbides of the kind associated with bainite [32], but was consistent with τ carbide, which is orthorhombic with lattice parameters $a = 14.8$, $b = 11.4$ and $c = 8.5$ Å, as found by Schissler [33]. Fig. 5(b) shows another brightfield image of carbides identified as silicon carbides of the type (Fe,Si)C_x [33]. This carbide is also orthorhombic with lattice parameters $a = 6.5$, $b = 7.7$ and $c = 10.4$ Å. Fig. 5(d) shows its selected area diffraction pattern.

3.2. Predictions of $V_{\gamma_r}^{\max}$ using the model

Eq. (2) for the calculation of the maximum volume fraction of bainite and Eq. (4) which is due to Khan and Bhadeshia, were used in conjunction with the curve illustrated in Fig. 6, to estimate $V_{\gamma_r}^{\max}$ for ADI as a function of chemical composition and heat treatment. There is good evidence that the amount of carbon that is precipitated from supersaturated ferrite during the bainite transformation, in the form of carbides, increases as the transformation temperature is reduced [34]. Indeed, this constitutes the mechanism for the transition from upper to lower bainite as the transformation temperature is reduced [34]. The profile illus-

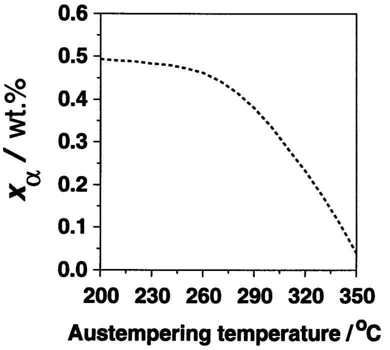

Fig. 6. Assumed concentration of carbon trapped in lower bainitic ferrite, in the form of carbides and in solution, as a function of temperature.

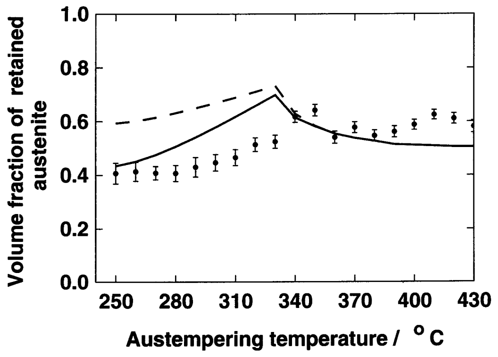

Fig. 7. Model (solid line) compared with experiments. The dashed line shows the predicted trend, assuming that carbon is not trapped within lower bainite. Austenitising temperature $T_\gamma = 950$ °C.

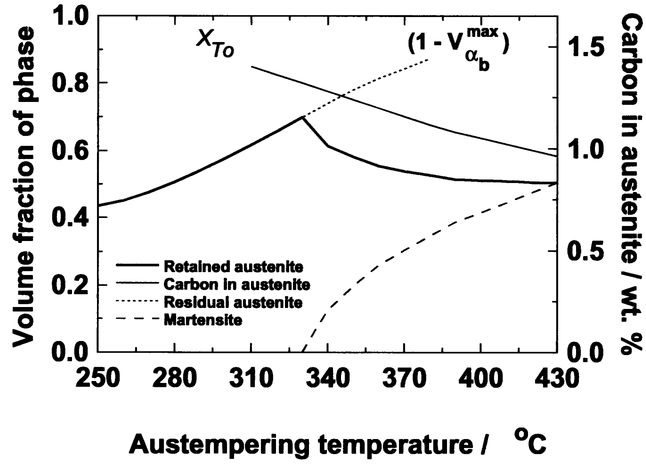

Fig. 8. Variation of the calculated volume fraction of retained austenite as a function of the austempering temperature (Fe–3.5C–2.5Si–0.55Mn–0.15Mo–0.31Cu wt.%). Austenitising temperature $T_\gamma = 950$ °C.

trated in Fig. 6 was therefore determined by optimising the fit between the measured retained austenite content and that calculated using Eq. (2) and Eq. (4). Predictions using Eq. (3) showed no significant difference with those using Eq. (4). The relevant computer program for carrying out these calculations was linked dynamically to MTDATA [35], which is a commercially available phase diagram calculation package of software. The role of MTDATA in the present work was to enable the estimation of the carbon concentration in the austenite, which is in equilibrium with graphite at the austenitisation temperature, $\bar{x}$, for any chemical composition and austenitising temperature.

The amount of carbon that is trapped in the lower bainite has been assumed to be the function illustrated in Fig. 6; the function was arrived at by fitting the calculated retained austenite content to experimental data of retained austenite found in the present work for temperatures < 350 °C. Without making this correction for carbon trapped in lower bainite, the model greatly overestimates $V^{\max}_{\gamma_r}$, as shown by the dashed line in Fig. 7. This figure also illustrates a set of predictions of $V^{\max}_{\gamma_r}$ as a function of the austempering temperature, for a cast iron austenitised at 950 °C and of chemical composition:

$$\mathrm{Fe} - 3.5\mathrm{C} - 2.5\mathrm{Si} - 0.55\mathrm{Mn} - 0.15\mathrm{Mo} - 0.31\mathrm{Cu}(\mathrm{wt.\%}).$$

There are two competing effects that explain the shape of the curve. The maximum fraction of bainite that can form increases as the transformation temperature is reduced, simply because of the slope of the T_0 curve. This, in turn, means that the carbon concentration x_{T_0} of the residual austenite is larger at lower temperatures. Carbon stabilises austenite and therefore, more of it would tend to be retained on cooling to ambient temperature.

The second, counteracting effect, is that the formation of bainite consumes austenite; less austenite is therefore available for retention as $V^{\max}_{\alpha_b}$ increases. This effect dominates once $(1 - V^{\max}_{\alpha_b})$ approaches $V^{\max}_{\gamma_r}$, at the lowest of transformation temperatures (Fig. 8). This is the reason for the peak occurring at the point where there is a change in the factor controlling the retention of austenite.

The model assumes a chemically homogeneous cast iron, which is never the case in practice. In order to validate the basic structure of the model, experiments were performed on samples homogenised for 3 days at 1000 °C before austempering. It is recognised that this treatment does not completely remove chemical segregation, but as illustrated in Fig. 9, it does lead to a more homogeneous microstructure.

4. Discussion

The predicted retained austenite content is found to be in reasonable agreement with that observed in the present work and is also quantitatively consistent with published results for segregated ductile irons [36–38]. As stated previously, the maximum volume fraction of

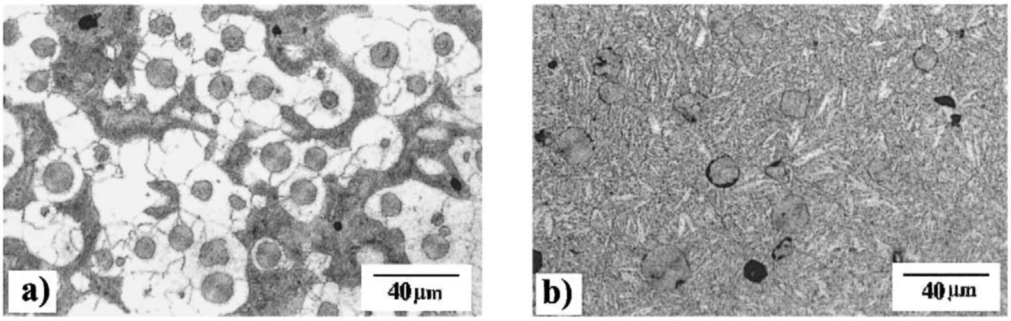

Fig. 9. Micrographs of ductile iron (a) As-cast, with nodules of graphite in a matrix which is a mixture of ferrite and pearlite. (b) As-homogenised for 3 days at 1000 °C, showing a more uniform microstructure consisting of graphite and martensite.

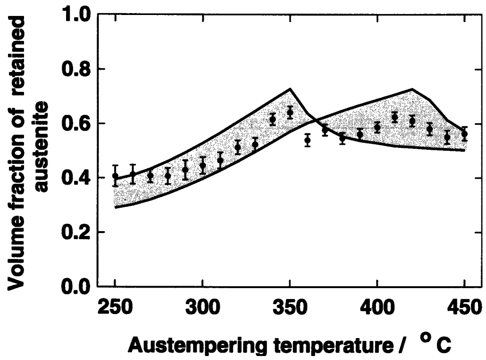

Fig. 10. Comparison between measured data and predicted retained austenite using the present model (unadjusted T_0) and a model with an empirical adjustment of 1.35 times x_{T_0}.

retained austenite depends on two competing effects: whereas an increase in the fraction of bainite raises the carbon concentration in the austenite, bainite also consumes austenite and hence, less remains to be retained. At low temperatures, it is the latter effect which dominates, leading to a fall in the amount of retained austenite.

For the lower transformation temperatures, the model seems to overestimate the maximum volume fraction of retained austenite. One reason for this might be the discrepancy between the T_0 curve and the measured carbon concentrations illustrated in Fig. 4. Thomson et al., [39] have, in their models, used an empirical factor to correct the T_0 value in order to obtain better agreement with certain kinetic data. In our case, this empirical factor, needed to fit x_{T_0} to the measured carbon concentration, would be 1.35. However, it is emphasised that this should be regarded as an upper limit to the uncertainty, since, as pointed out earlier, X-ray measurements tend to overestimate the carbon concentration of austenite in bainitic microstructures. Fig. 10 is therefore a comparison of measured data against a shaded region defined by calculations using the unadjusted T_0 curve and one with the empirical adjustment. It appears, therefore, that the major reason for any discrepancy between theory and experiment is the inhomogeneous distribution of carbon in the residual austenite.

5. Conclusions

There are many results in the literature [40–43] and new results have been obtained in the present work, which show that the maximum content of retained austenite that can be obtained in austempered ductile cast iron peaks as a function of the isothermal transformation temperature.

It has been demonstrated that this behaviour can be understood in terms of two competing effects. The first is that the formation of bainite enriches the residual austenite so that more austenite is retained on cooling to ambient temperature. The second effect dominates at the lower transformation temperatures because the very formation of bainite leaves less austenite available for retention.

Consistent with the observation of lower bainite, it has been necessary to assume that the amount of carbon that is trapped within bainitic ferrite, as carbides and in solution, increases as the transformation temperature is reduced below 350 °C.

Acknowledgements

The authors are grateful to Professor D.J. Fray for the provision of laboratory facilities at the University of Cambridge. One of the authors (M.A.Y.) would like to thank the National Council of Science and Technology of Mexico (CONACYT) for a scholarship.

References

[1] N. Darawish, R. Elliott, Mater. Sci. Technol. 9 (1993) 572.
[2] F.R. Wilson, R.A. Harding, BCIRA Report No. 1783, Birmingham, UK, 1989.
[3] R.F. Hehemann, in: V.F. Zackay, H.I. Aaronson (Eds.), Phase Transformations, ASM, Metals Park, OH, 1970, p. 397.

[4] H.K.D.H. Bhadeshia, D.V. Edmonds, Acta Metall. 28 (1980) 1265.
[5] H.K.D.H. Bhadeshia, D.V. Edmonds, Acta Metall. 28 (1980) 1103.
[6] H.K.D.H. Bhadeshia, D.V. Edmonds, Metall. Trans. 10A (1979) 895.
[7] M.A. Yescas, H.K.D.H. Bhadeshia, D.J.C. MacKay, Mater. Sci. Eng. A311 (2001) 162.
[8] B.D. Cullity, Elements of X-ray Diffraction, Addison-Wesley, Reading, MA, 1978, p. 324.
[9] D.J. Dyson, B. Holmes, J. Iron Steel Inst. 208 (1970) 469.
[10] D.J. Moore, T.N. Rouns, K.B. Rundman, AFS Trans. 94 (1986) 255.
[11] N. Darawish, R. Elliott, Mater. Sci. Technol. 9 (1993) 572.
[12] H.K.D.H. Bhadeshia, D.V. Edmonds, Metall. Trans. 10A (1979) 895.
[13] S.A. Khan, H.K.D.H. Bhadeshia, Mater. Sci. Eng. A129 (1990) 257.
[14] D.P. Koistinen, R.E. Marburger, Acta Metall. 7 (1959) 59.
[15] H.K.D.H. Bhadeshia, A.R. Waugh, Acta Metall. 30 (1982) 775.
[16] H. Niesawaag, J.W. Nijhof, Proceedings of the International Symposium on Physical Metallurgy of Cast Iron, vol. 34, 1985, p. 411.
[17] M.N. Ahmadabadi, Metall. Mater. Trans. A28 (1997) 2159.
[18] L.C. Chang, Scr. Mater. 39 (1998) 35.
[19] R.L. Houillier, G. Begin, A. Dubè, Metall. Trans. 2A (1971) 2645.
[20] H.K.D.H. Bhadeshia, Acta Metall. 28 (1980) 1265.
[21] K.B. Rundman, R.C. Klug, AFS Trans. 90 (1982) 499.
[22] D.A. Harris, B. Tech, R.J. Maitland, J. Iron Steel 208 (1970) 53.
[23] S.J. Matas, R.F. Hehemann, Trans. AIME 221 (1961) 179.
[24] F.B. Pickering, Transformation and hardenability in steels, in: Climax Molybdenum, 1967, p. 109.
[25] D.H. Huang, G. Thomas, Metall. Trans. 8A (1977) 1661.
[26] B.P.J. Sandvik, Metall. Trans. 13A (1982) 777.
[27] E. Dorazil, High Strength Austempered Ductile Cast Iron, Ellis Horwood Ltd, West Sussex, UK, 1991, p. 43.
[28] W.J. Dubensky, K.B. Rundman, AFS Trans. 93 (1985) 389.
[29] M.N. Ahmadabadi, Metall. Mater. Trans. A29 (1998) 2297.
[30] C.S. Roberts, B.L. Averbach, M. Cohen, Trans. ASM 45 (1957) 576.
[31] M.K. Kang, J.L. Sun, Q.M. Yang, Metall. Trans. 21A (1990) 853.
[32] H.K.D.H. Bhadeshia, Bainite in Steels, Institute of Materials, London, 1992, p. 76.
[33] J.M. Schissler, J. Arnould, G. Metauer, Mem. Sci. Rev. Metal. 6 (1975) 779.
[34] M. Takahashi, H.K.D.H. Bhadeshia, Mater. Sci. Technol. 6 (1990) 592.
[35] MTDATA, Metallurgical and Thermomechanical Databank, National Physical Laboratory, Teddington, Middlesex, UK, 1995.
[36] M. Grech, J.M. Young, AFS Trans. 98 (1990) 345.
[37] H. Bayati, R. Elliott, Mater. Sci. Technol. 11 (1995) 118.
[38] K.B. Rundman, D.J. Moore, K.L. Hayrynen, W.J. Dubensky, T.N. Rouns, J. Heat Treat. 5 (1988) 79.
[39] R.C. Thomson, J.S. James, D.C. Putman, Mater. Sci. Technol. 16 (2000) 1412.
[40] S.E. Stenfors, J. Storesun, R. Sandstrom, Second International Conference on Austempered Ductile Iron, University of Michigan, 1986, p. 227.
[41] M.M. Shea, E.F. Ryntz, AFS Trans. 94 (1986) 683.
[42] W.S. Zhou, Q.D. Zhou, S.K. Meng, Cast. Met. 2 (1993) 69.
[43] I. Schmid, A. Schuchert, Z. Metallkd. 78 (1987) 871.